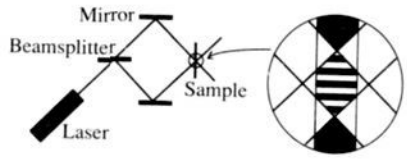

Figure 1. Crossed-beam irradiation generates interference fringes that are recorded in the sample through photochemistry. The resulting grating can then diffract one of the beams into the other.

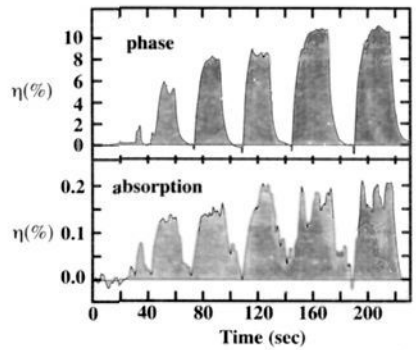

Figure 2. Diffraction efficiency due to phase (refractive index) and absorption for **1** in its nematic phase (with photoinitiator) at 130 °C. Crossed-beam irradiation was begun at $t = 0$ s, and an electric field was applied intermittently, corresponding to the sharp increases in efficiency.

interference fringes that are recorded in the sample through its photochemistry (Figure 1). Simultaneous reading is accomplished in PIH by chopping one beam and measuring the diffracted intensity with a photodiode. In PMH, one beam is phase-modulated and the resulting beat signal is detected in both beams. In our experiments, the 647-nm line of a Spectra Physics 2020 Kr ion laser was used. The monomer, with a small amount of dissolved photoinitiator,[8] was drawn by capillary action into a 6-μm thermostated cell made from indium–tin oxide coated glass (from Applied Films Laboratory). No aligning surface treatments were used for these experiments.[4]

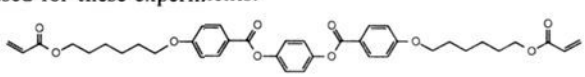

1 (C 108 S (88) N 155 I)

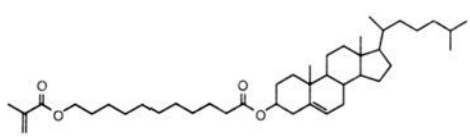

2 (C 53.2 S 54.8 Ch 64.4 I)

Results from a representative PMH experiment with **1** in its nematic liquid crystalline phase at 130 °C are shown in Figure 2. The PMH experiment allows separate detection of diffraction due to phase and absorption effects, and plots for both are shown. A relatively weak phase diffraction was observed during the initial photopolymerization, and a dramatic 25-fold increase was observed upon application of an alternating electric field (100 V, 1 kHz) to the sample. The diffraction efficiency rose from 0.4% without the field to a peak of 11% with the field on.[9] The reversibility of this modulation was also demonstrated.[10] The sign of the modulation indicates that the regions of destructive interference have the larger refractive index, which is consistent with the model stated above that depicts the liquid crystalline monomer in these regions to be aligned with the field. The diffracted intensity due to absorption was about 50 times weaker than the phase signal.

Similar results were obtained when the photopolymerization was carried out under an applied electric field followed by *removal* of the field. With this procedure, diffraction efficiencies up to 18% were observed, although the modulation was somewhat reduced, due to more efficient diffraction during the initial polymerization.

Modulation was also observed with **2** in its cholesteric phase at 58 °C; however, the increases were very small (10–30%). That **2** gives rise to lower modulation is not surprising, since the relative lack of unsaturation should lead to smaller birefringence for this liquid crystal. In addition, the side-chain polymer of **2** may possess significant fluidity, since the mesogens are only anchored at one end. The cross-linked network polymer of **1** has been shown to remain oriented in a smectic phase up to 300 °C.[5]

In conclusion, we have demonstrated that a liquid crystalline monomer, **1**, performs well as a highly efficient, switchable optical recording medium.[11] Even at this preliminary stage, this medium has the properties necessary for application in holographic displays, spatial light modulators, and holographic associative memories.[12] Work is continuing toward the optimization of these media.

Acknowledgment is made to the donors of the Petroleum Research Fund, administered by the American Chemical Society, and to the Camille and Henry Dreyfus Foundation New Faculty Award Program, for partial support of this work.

(7) Pinsl, J.; Gehrtz, M.; Reggel, A.; Bräuchle, C. *J. Am. Chem. Soc.* **1987**, *109*, 6479–6486. Gehrtz, M.; Pinsl, J.; Bräuchle, C. *Appl. Phys. B* **1987**, *43*, 61–77.

(8) A sample of an appropriate-wavelength cyanine borate photoinitiator was provided by Mead Imaging Corporation. For initiator photochemistry, see: Chatterjee, S.; Davis, P. D.; Gottschalk, P.; Kurz, M. E.; Sauerwein, B.; Yang, X.; Schuster, G. B. *J. Am. Chem. Soc.* **1990**, *112*, 6329–6338.

(9) The switching occurs on a time scale of about 2 s.

(10) The durability of the switching medium can presumably be improved by reading the hologram with a wavelength of light that is not absorbed by the photoinitiator. We have not yet carried out these experiments.

(11) High sensitivity may also be expected, since photopolymerization has been shown to be faster in liquid crystalline phases.[6] Our experiments have not yet addressed this aspect.

(12) Birge, R. R. *Annu. Rev. Phys. Chem.* **1990**, *41*, 683–733.

RLi·LiCuR$_2$ Dimers: An Explicit Structural Alternative to "Higher Order" Homocuprates

James P. Snyder,* Gregory E. Tipsword, and Dale P. Spangler

Drug Design, Searle Research and Development
4901 Searle Parkway, Skokie, Illinois 60077

Received April 19, 1991

Appearance of the now-classic Gilman reagents[1] in 1952 spawned an era of organocopper chemistry that dominates transition-metal-directed carbon–carbon bond formation today.[2-4] Based on the ratio of alkyllithium to methylcopper, a range of stoichiometries[5-7] and reactivities[8] can be observed for the lithium–copper reagents. Although a list of informative X-ray structures is growing,[9-16] a clear correspondence between chem-

(1) Gilman, H.; Jones, P. H.; Woods, L. A. *J. Org. Chem.* **1952**, *17*, 1630.

(2) Collman, J. D.; Hegedus, L. S. *Principles and Applications of Organo-Transition Metal Chemistry*; University Science Books: Mill Valley, CA, 1980; p 544.

(3) Posner, G. H. *An Introduction to Synthesis Using Organo-Copper Reagents*; Wiley: New York, 1980.

(4) Lipshutz, B. H. *Synthesis* **1987**, 325.

(5) Ashby, E. C.; Watkins, J. J. *J. Chem. Soc., Chem. Commun.* **1976**, 784.

(6) Ashby, E. C.; Watkins, J. J. *J. Am. Chem. Soc.* **1977**, *99*, 5312.

(7) Lipshutz, B. H.; Kozlowski, J. A.; Breneman, C. M. *J. Am. Chem. Soc.* **1985**, *107*, 3197.

(8) Lipshutz, B. H.; Wilhelm, R. S.; Kozlowski, J. A. *Tetrahedron* **1984**, *24*, 5005.

(9) Edwards, P. G.; Gellert, R. W.; Marks, M. W.; Bau, R. J. *J. Am. Chem. Soc.* **1982**, *104*, 2072.

(10) Eaborn, C.; Hitchcock, P. B.; Smith, J. D.; Sullivan, A. C. *J. Organomet. Chem.* **1984**, *263*, C23.

0002-7863/92/1514-1507$03.00/0

Table I. Relative Energies and Partial Geometries for the PRDDO-Optimized Isomers of $Li_2CuMe_3 \cdot (H_2O)_2$

	r(Cu···CLi_2), Å	r(Cu–CH_3), Å	θ(C–Cu–C), deg	ΔE_{rel}, kcal/mol[a-c] 3-21G/ ECP(DZ)	LANL1DZ	6-31G*/ ECP(DZ)	LANL1DZ/ MP2
3	3.718	1.967	174.2	0.0	0.0	0.0	0.0
	3.708[d]	2.090	178.7				
4	3.280	1.964	163.2	13.9	13.5	14.2	11.8
5	2.778	1.981	162.5	26.7	26.3	26.5	25.7
6	3.115	1.969	172.7	29.5	27.0	27.8	25.9
7	3.141	1.959	175.1	25.1	25.0	25.5	21.0
8	1.985	2.195	110.2	19.8	19.6	18.3	19.1
			124.9				
9	2.202	2.046	128.2	16.2	17.2	16.9	17.6
			115.9				

[a] The 3-21G/ECP(DZ) basis set is a hybrid composed of the 3-21G[46] contraction for first row atoms and the Los Alamos ECP+DZ for copper.[47] LANL1DZ utilizes the D95V basis[48] coupled to the latter. The 6-31+G*/ECP(DZ) prescription employed a standard 6-31G* basis supplemented by diffuse orbitals[49] on carbon and oxygen. Electron correlation effects were calculated with Møller–Plesset theory[50] carried out to second order (MP2). [b] All calculations used the Gaussian 88 program[27] absolute energies for **3** (au): 3-21G/ECP(DZ), −334.665 43; LANL1DZ, −336.176 93; 3-21+G*/ECP(DZ), −336.202 14; LANL1DZ/MP2, −336.927 74. [c] To verify that the optimization methods employed in this work are capable of treating Cu(I) organometallics, three divalent linear R_2Cu^+ species were geometry-refined (X-ray, PRDDO, LANL1DZ): r(Cu—CH_3) 1.935,[51] 1.982, 2.086 Å; r(Cu—C_6H_5) 1.925,[51] 1.986, 2.040 Å; r(Cu–N(imidazole)) 1.879,[52] 1.939, 2.005 Å. Each calculation expands R—Cu—R from a 160° start to 176—180° in agreement with the crystal structures. A fragment of a trivalent Cu(I) dimer, $[Cu_2(HL—H)(MeCN)_2][ClO_4]_2$,[53] was treated similarly: r_1(Cu—N) 1.959, 1.969, 2.072 Å; r_2(Cu–N) 1.975, 1.989, 2.072 Å; r(Cu—N(≡C—Me)) 1.507, 1.934, 2.268 Å. [d] See Ref. 32.

ically active species and three-dimensional structure has yet to be established. The simplest Gilman constitution, $LiCuR_2$, is an exception. The early proposal[17] for a lower order dimer (**1**) has been confirmed by molecular weight determination[6] and NMR spectroscopy[18] and amply demonstrated by X-ray crystallography.[12,14-16]

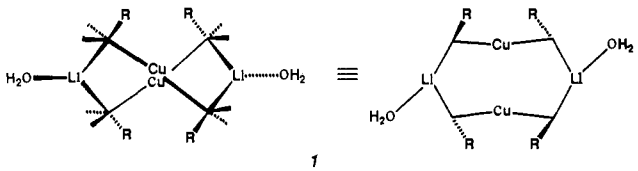

1

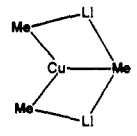

2

The first member in the series of so-called higher order organocuprates, Li_2CuR_3 (R = Ph), was deduced on the basis of chemical evidence.[19] Ebullioscopic molecular weight measurements indicate a monomeric structure for Li_2CuMe_3,[6] while NMR illustrates the presence of two different types of R groups in solution.[5,6,20] A possible structure for Li_2CuMe_3 has been depicted[5] as in **2**. A presumably related cyano variant, $Li_2Cu(CN)R_2$, the source of rich synthetic application,[4,8] is explicitly regarded in some quarters as a formal dianionic salt with three ligands covalently bonded to copper.[8,21] In the present communication, the structure of partially solvated Li_2CuMe_3 is explored theoretically. The concept of "higher order" as it applies to copper in homocuprate reagents is consequently called into question.

Structures **3–9** and their symmetric C–CH_3 conformations were considered as candidates for Li_2CuMe_3 in ethereal solvent. Each

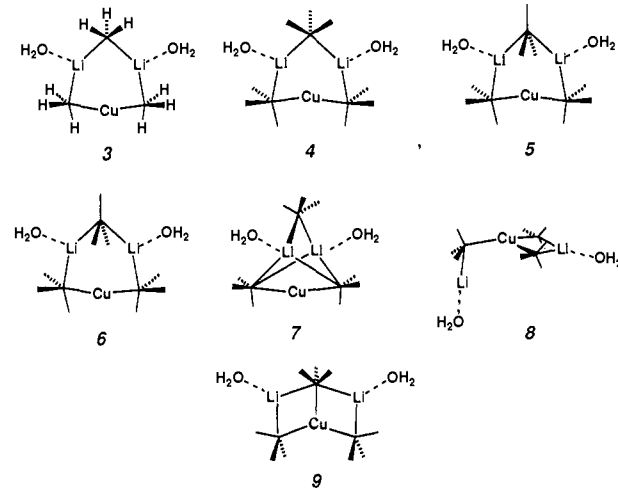

3 **4** **5** **6** **7** **8** **9**

was embellished with two molecules of water as solvent surrogates. Trigonal planarity for annular lithium was adapted in concordance with X-ray results.[14,22] The constructs were geometry-optimized with PRDDO,[23-26] the final structures being subjected to energy evaluations with three split-valence basis sets in the Gaussian 88[27] framework. Structures **3**, **8**, and **9** were also refined with the LANL1DZ basis set.[28] Table I summarizes the results and

(11) Hope, H.; Oram, D.; Power, P. D. *J. Am. Chem. Soc.* **1984**, *106*, 1149.
(12) Koten, G. v.; Jastrzebski, J. T. B. H. *J. Am. Chem. Soc.* **1985**, *107*, 697.
(13) Olmstead, M. M.; Power, P. P. *J. Am. Chem. Soc.* **1989**, *111*, 4135.
(14) Lorenzen, N. P.; Weiss, E. *Angew. Chem., Int. Ed. Engl.* **1990**, *29*, 300.
(15) Olmstead, M. M.; Power, P. P. *Organometallics* **1990**, *9*, 1720.
(16) Olmstead, M. M.; Power, P. P. *J. Am. Chem. Soc.* **1990**, *112*, 8008.
(17) Pearson, R. G.; Gregory, C. D. *J. Am. Chem. Soc.* **1976**, *98*, 4098.
(18) Koten, G. v.; Noltes, J. G. *J. Am. Chem. Soc.* **1979**, *101*, 6593.
(19) House, H. O.; Koepsell, D. G.; Campbell, W. J. *J. Org. Chem.* **1972**, *37*, 1003.
(20) Bertz, S. H.; Dabbagh, G. *J. Am. Chem. Soc.* **1988**, *110*, 3668.
(21) Lipshutz, B. H.; Sharma, S.; Ellsworth, E. L. *J. Am. Chem. Soc.* **1990**, *112*, 4032.
(22) Lappert, M. F.; Slade, M. J.; Singh, A.; Atwood, J. L.; Rogers, R. D.; Shakir, R. *J. Am. Chem. Soc.* **1983**, *105*, 302.
(23) Halgren, T. A.; Kleier, D. A.; Hall, J. H., Jr.; Brown, L. D.; Lipscomb, W. N. *J. Am. Chem. Soc.* **1978**, *100*, 6595.
(24) Marynick, D. S.; Lipscomb, W. N. *Proc. Natl. Acad. Sci. U.S.A.* **1982**, *79*, 1341.
(25) Marynick, D. S.; Axe, F. U.; Kirkpatrick, C. M.; Throckmorton, L. *Chem. Phys. Lett.* **1983**, *99*, 406.
(26) Graham, G.; Richtsmeier, S.; Dixon, D. A. *J. Am. Chem. Soc.* **1980**, *102*, 5759.
(27) Frisch, M. J.; Head-Gordon, M.; Schlegel, H. B.; Raghavachari, K.; Binkley, J. S.; Gonzalez, C.; Defrees, D. J.; Fox, D. J.; Whiteside, R. A.; Seeger, R.; Melius, C. F.; Baker, J.; Martin, R. L.; Kahn, L. R.; Stewart, J. J. P.; Fluder, E. M.; Topiol, S.; Pople, J. A. *Gaussian 88*; Gaussian, Inc.: Pittsburgh, PA, 1988.

demonstrates that quantum mechanical methodology predicts Cu(I) structures semiquantitatively.

The Li_2CuMe_3 structures fall into the two categories popularly characterized as lower and higher order. The first lower order set, **3–7**, contains a slightly nonlinear dimethylcopper unit coupled to a dilithium–methyl bridge. Both σ and π Li–C–Li moieties are represented. Structures in this group incorporate a long Cu···$CH_3(Li_2)$ bond ($\geq$2.8 Å). The second set, **8** and **9**, consists of higher order cuprates with trivalent "dianionic" copper. The pyramidal species **9** corresponds to topology **2**. While not all of these structures may correspond to stationary points, they do represent PRDDO minima with the indicated symmetry.[28,29]

Relative calculated energies favor divalent copper-containing rings by a wide margin (Table I).[28,30,31] Cycle **3** with the greatest separation between bridging CH_3 and Cu (3.72 Å) falls into the deepest energy well.[32] In accord with low-temperature NMR (−136 °C, Me_2O),[5,6] the two different methyl groups are in a ratio of 2:1. Interestingly, torsional disposition of the Cu–CH_3 fragments is identical to that observed in the X-ray for **1** (R = $SiMe_3$, Me_2S solvate; i.e., the Li–C–R fragment is nearly linear) as is the C–Cu–C bond angle (174.2° (calcd) vs 171.5 and 173.8° (obsd)).[15] The overall topology of six-ring **3** is strikingly similar to that found for lithium amide trimers both experimentally[33,34] and theoretically.[35] The structure can be regarded as a ring-contracted mimic of dimer **1**. However, the unique CH_3 center buttressed by two solvated lithium atoms can be expected to demonstrate differential reactivity by comparison with the methyls of $(LiCuMe_2)_2$ **1**. Consistently, Li_2CuMe_3 has been shown to methyl-displace halides and to promote 1,4 conjugate addition in a manner superior to MeLi or other $Li_xCu_yMe_z$ combinations.[8,36,37]

Can the six-membered ring **3** accommodate the enhanced and selective reactivity profile? It has been proposed that dimer **1** initiates its chemistry through the agency of a π complex,[38,39] several of which are reported to have been observed by NMR.[40–42]

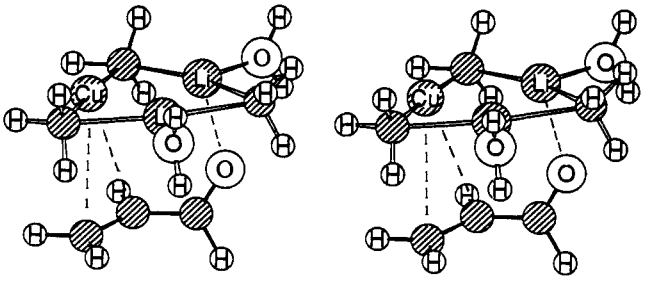

Figure 1. Complex of acrolein and the MeLi·Li_2CuMe_3 dimer **3**; stereoview. The orientation of the two supermolecule components was PRDDO-optimized by assuming a variable (O)CH–$CH(CH_2)$ torsion and otherwise fixed internal variables.

Similarly, the divalent copper center in **3** can in principle complex to a reaction partner as a preliminary to delivery of methyl. A series of complexes incorporating α,β-unsaturated carbonyls has been examined with PRDDO. One optimized structure for acrolein complexed to **3** by means of C=O···Li and $C{=}CH_2$···Cu interactions, for example, is depicted in Figure 1. The composite accords with the existence of lithium-bound carbonyl in the NMR.[40–42] Straightforward 1,4 conjugate addition can follow by transfer of CH_3(Cu, Li) to $CH_2{=}C$. 1,2-Addition by the distal CH_3(Li, Li) in Figure 1 is stereoelectronically less favorable. It is prudent to recall that direct observation of aggregates in solution is no guarantee that they lie on a reaction pathway of interest. Recent studies elegantly demonstrate that adducts of lower stability can readily serve as channels to product.[43,44] Accordingly, the complex depicted in Figure 1, while an energy minimum, is several kilocalories per mole higher in energy than C=O···Li structures with the terminal methylene directed away from cycle **3**. Geometrics and stereoelectronic details for the modeled complex, isomeric orientations, and mechanistic implications will be reported separately.

In conclusion, monomeric Gilman reagents characterized by a 2:1 ratio of RLi to CuR, e.g., Li_2CuMe_3, are predicted to prefer a monocyclic ring containing a near-linear R–Cu–R fragment and divalent copper, **3**, rather than a higher order Cu tricoordinate species such as **8** and **9**. Cycle **3** is simply an aggregate of the methyl and dimethylcopper anions bridged by a pair of lithium cations, namely, a dimer of MeLi and $LiCuMe_2$. This view emphasizes the possible structural similarity of Li_2CuMe_3 and dimer **1** $(Li_2CuR_2)_2$,[45] underscores their participation in a facile exchange equilibrium,[5,6] and intimates a unified explanation for the observed variation in reactivity. It likewise suggests the existence of an expanded class of organocopper reagents based on the structural principles inherent in **3**.

(28) As an independent check on the symmetry-constrained, cyclically optimized[25,26] PRDDO structures, **3** and **9** without waters were reoptimized at the LANL1DZ level (cf. Table I) by the method of gradients.[27] Bicyclic **9** is either not a stationary point on the LANL1DZ surface or resides in a very shallow energy well, since it reverts to cycle **3** upon full relaxation. Fixing the unique Cu–CH_3 bond length to 2.2 Å leads to optimized **9** destabilized by 15.5 and 24.5 kcal/mol relative to **3** (with and without H_2O, respectively). Unsolvated higher order **8** explodes to Cu–CH_3 and the cyclic dimer of methyllithium.[29] Constraining the symmetry-related Cu–C bonds to 2.1 Å yields geometry-optimized **8** less stable than **3** by 38.5 kcal/mol. In a further set of optimizations to assess possible solvation effects, **3** with two symmetrical waters on each Li was compared with **8** $(Li(H_2O)_3/Li'(H_2O)$ and $Li(H_2O)_2/Li'(H_2O)_2)$. The LANL1DZ//PRDDO energy evaluation finds the former more stable by 17.6 and 9.3 kcal/mol, respectively.

(29) Kaufmann, E.; Raghavachari, K.; Reed, A. E.; Schleyer, P. v. R. *Organometallics* **1988**, *7*, 1597.

(30) The ΔE_{rel} invariance upon supplementation of C and O with diffuse functions (6-31+G,* Table I) eliminates orbital superposition as a source of error (BSSE)[31] and confirms the result to be basis set independent. Electron correlation effects (MP2) are likewise unimportant.

(31) Bachrach, S. M.; Streitwieser, A., Jr. *J. Am. Chem. Soc.* **1984**, *106*, 2283.

(32) Internal variables for the planar global minimum **3** include (PRDDO, LANL1DZ; Å, deg) the following: Cu–C 1.967, 2.090; Cu···C 3.718, 3.708; Li–C(Cu) 1.994, 2.274; Li–C(Li) 2.121, 2.166; C–Cu–C 174.2, 178.7; C–Li–C 161.6, 148.1; Li–C–Li 75.1, 84.7; Li–C–Cu 73.8, 73.6; O–Li–C(Cu) 97.3, 102.0.

(33) Rogers, R. D.; Atwood, J. L.; Gruning, R. *J. Organomet. Chem.* **1978**, *157*, 229.

(34) Barr, D.; Clegg, W.; Mulvey, R. E.; Snaith, R. *J. Chem. Soc., Chem. Commun.* **1984**, 285.

(35) Sapse, A.-M.; Kaufmann, E.; Schleyer, P. v. R.; Gleiter, R. *Inorg. Chem.* **1984**, *23*, 1569.

(36) Still, W. C.; Macdonald, T. C. *Tetrahedron Lett.* **1976**, 2659.

(37) Ashby, E. C.; Lin, J. J. *J. Org. Chem.* **1977**, *42*, 1099; **1977**, *42*, 2805.

(38) Ullenius, C.; Christenson, B. *Pure Appl. Chem.* **1988**, *60*, 57.

(39) Bergdahl, M.; Lindstedt, E.-L.; Nilsson, M.; Olsson, T. *Tetrahedron* **1989**, *45*, 535.

(40) Hallinemo, G.; Olsson, T.; Ullenius, C. *J. Organomet. Chem.* **1985**, *282*, 133.

(41) Christenson, B.; Olsson, T.; Ullenius, C. *Tetrahedron* **1989**, *45*, 523.

(42) Bertz, S. H.; Smith, R. A. J. *J. Am. Chem. Soc.* **1989**, *111*, 8276.

(43) Landis, C. R.; Harpern, J. *J. Am. Chem. Soc.* **1987**, *109*, 1746.

(44) Hay, D. R.; Song, Z.; Smith, S. G.; Beak, P. *J. Am. Chem. Soc.* **1988**, *110*, 8145.

(45) The calculated dimerization energy for **3** from $CuMe_2^-$, tetrahedral $Li(OH2)_4^+$, and $(MeLi)_2{\cdot}(OH_2)_2$ is −42.2 kcal/mol (LANL1DZ basis; cf. Table I). The comparable association of MeLi to dimer is −41.7 kcal/mol (6-31G).[29]

(46) Binkley, J. S.; Pople, J. A.; Hehre, W. J. *J. Am. Chem. Soc.* **1980**, *102*, 939.

(47) Hay, P. J.; Wadt, W. R. *J. Chem. Phys.* **1985**, *82*, 270; **1985**, *82*, 284; **1985**, *82*, 299.

(48) Dunning, T. H.; Hay, P. J. *Modern Theoretical Chemistry*; Miller, W., Ed.; Plenum Press: New York, 1976; pp 1–28.

(49) Clark, T.; Chandrasekhar, J.; Spitznagel, G. W.; Schleyer, P. v. P. *J. Comput. Chem.* **1983**, *3*, 294.

(50) Binkley, J. S.; Pople, J. A. *Int. J. Quantum Chem.* **1975**, *9*, 229, and references therein.

(51) Hope, H.; Olmstead, M. M.; Power, P. P.; Sandell, J.; Xu, X. *J. Am. Chem. Soc.* **1985**, *107*, 4337.

(52) Sorrell, T. N.; Jameson, D. L. *J. Am. Chem. Soc.* **1983**, *105*, 6013.

(53) Dagdigian, J. V.; McKee, V.; Reed, C. A. *Inorg. Chem.* **1982**, *21*, 1332.

Acknowledgment. We are appreciative to Dr. Bryant Rossiter (Brigham Young University) for stimulating our interest in organocuprate chemistry. We are likewise grateful to Drs. James Behling and John Ng (Searle), Gary Posner (Johns Hopkins University), and Peter Beak (University of Illinois) for enlightening discussion. Drs. Marilyn Olmstead and Philip Power (University of California, Davis) graciously provided unpublished X-ray coordinates.

Registry No. Li_2CuMe_3, 61278-42-0.

Extension and Completion of the Periodic Table

Leland C. Allen

Department of Chemistry, Princeton University
Princeton, New Jersey 08544

Received May 28, 1991
. Revised Manuscript Received December 2, 1991

In spite of—or because of—its everyday familiarity, the periodic table possesses a number of puzzling and infrequently addressed features. (1) What is the origin of its diagonal line separating metals from nonmetals? (2) It is far from periodic: it has long been recognized that as one descends a group in the p-block the character of the elements becomes increasing metallic. The chemistry of carbon is quite different from the chemistry of lead. (3) Why do the fluorides of N, O, F, Cl, Br, He, Ne, Ar, and Kr not reach oxidation states equal to the number of their valence electrons? (4) It is our principal guide in anticipating which of the three types of bonding, covalent, metallic, or ionic, will form between atoms. But it provides no definition of these bond types, nor a way to differentiate between them. (5) It is the most powerful instrument for organizing chemical phenomena but it does not contain any information about the energy of atoms, even though everyone knows that energy is the central parameter for describing the structure of matter.

It is clear that something is missing, and this appears to be an historical accident dating from the time when Bohr provided the physical underpinning of the periodic table by defining electronic configurations.[1] In chemical terms, the periodic table is a sequence of groups whose atoms have common properties and behavior, and since a two-dimensional array displays all of the atoms, it superficially appears complete. Physicists, however, see it as a collection of valence electron configurations that depict the properties of atomic shell structure. The quantum numbers n and l introduced by Bohr[1] label blocks of elements and indicate orbital size and shape, but their primary role is to specify *energy*. When orbital occupancy is taken into account, it immediately follows that configuration energy (CE), the average one-electron valence shell energy of a ground-state free atom, is the missing third dimension:

$$\mathrm{CE} = (a\epsilon_s + b\epsilon_p)/(a + b) \qquad (1)$$

where a, b are occupanices and ϵ_s, ϵ_p the s and p ionization potentials for spherical atoms of the representative elements; for the d-block transition elements, $\epsilon_p \rightarrow \epsilon_d$ of the $n - 1$ shell and b is its valence region occupancy.[2-4] CE possesses another energy level related property that is of equal importance to that expressed in eq 1: it is strongly correlated with the spacings of the one-electron energy levels of the atom in question. Large CE goes with large energy level separations, thus making a close connection between the magnitude of CE and the density of states in solids and molecules.[4] This correlation follows immediately from the fact that the effective potential seen by an electron in an atom is funnel-shaped: steeper and deeper funnels have more widely spaced energy levels.

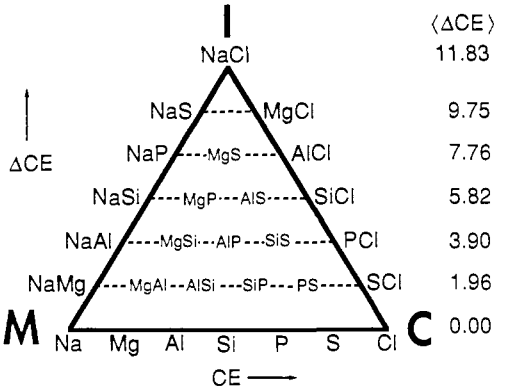

Figure 1. Quantification of a Van Arkel-Ketelaar triangle illustrated by second row atoms: M, metallic; I, ionic; C, covalent. The horizontal axis is the $n = 3$ row of the periodic table and spans a CE range from 5.14 (Na) to 16.97 eV (Cl). ⟨ΔCE⟩ is the average CE difference for pairs of atoms in each horizontal line through the triangle (the stoichiometry of the generic binary combinations of atoms has been suppressed). (The smaller size of lettering inside the triangle was employed for pictorial clarity and has no chemical significance.)

CE answers the questions posed earlier. (1) Values generated by eq 1[2,3] precisely define the metalloid band (B, Si, Ge, As, Sb, and Te) associated with the metal/nonmetal diagonal line: all elements to the right of the metalloids have higher CEs and are nonmetals; all those to the left have lower CEs and are metals. The band itself is a region of nearly constant CE. (2) Metalization down a group occurs because the size of the atoms is increasing; therefore, both the magnitude of the average valence energy level and the spacings of the levels are decreasing. Bonding directionality is being lost because the s, p, and d levels are becoming nearly degenerate, allowing mixing in many combinations. These changes are quantified by CE[4]. (3) The oxidation-state limitations of N, O, F, Cl, and Br are explained by their CEs: these and the noble gas atoms He, Ne, Ar, and Kr have the highest CEs in the periodic table and some fraction of their valence electrons is held too tightly to engage directly in bonding. Because of their high CEs, they have a correspondingly large energy gap to the first available unoccupied level, likewise discouraging bonding. (4) Quantification of Van Arkel-Ketelaar triangles[3,5] by CE and ΔCE helps interpret what the periodic table is telling us and permits one to differentiate metallic, ionic, and covalent bonding (Figure 1). Particularly interesting materials are found near the centers of each leg of the triangle: the metalloids (as well as III-V and II-VI semiconductors) along the M-C leg, polymeric compounds (e.g., AlF_3) along I-C, and Zintl phases along M-I.

It is the hypothesis of this communication that CE uniquely qualifies as an intrinsic third coordinate which completes the periodic table. A principle function of the periodic table has always been to present a two-dimensional array against which many properties have been correlated. These include the following: atomic radii,[6] polarizabilities, ionization potentials, acid-base behavior, electronegativities, boiling and melting points, diamagnetic susceptibilities, magnetic moments, field gradients at the nucleus, crystal structures, electrical and thermal conductivities, semiconductor energy gaps, etc.[7] Many of these have been presented pedagogically in texts as periodic table third dimensions, but they are actually part of its vast collection of correlative

(1) Bohr, N. *Nature* **1923**, *112*, 29.
(2) Supplemental material attached.
(3) Allen, L. C. *J. Am. Chem. Soc.* **1989**, *111*, 9003. The new viewpoint presented here is an extension and generalization of the 1989 article.
(4) Allen, L. C. Configuration Energies for the Elements and Their Use in Explaining the Structure of Matter. *J. Am. Chem. Soc.*, in press.
(5) Van Arkel, A. E. *Molecules and Crystals in Inorganic Chemistry*; Interscience: New York, 1956. Ketelaar, J. A. A. *Chemical Constitution, An Introduction to the Theory of the Chemical Bond*, 2nd ed.; Elsevier: New York, 1958.
(6) Radius can be shown to be inversely proportional to CE.[4]
(7) Emsley, J. *The Elements*; Clarendon Press: Oxford, UK, 1989.

0002-7863/92/1514-1510$03.00/0